CONDENSATION HEAT TRANSFER OF R-22 AND R-410A IN FLAT ALUMINUM MULTI-CHANNEL TUBES

Nae-Hyun Kim, Professor, Department of Mechanical Engineering, University of Incheon, Incheon, Korea
Ho-Jong Jeong, Graduate student, University of Incheon, Incheon, Korea
Jin-Pyo Cho, Graduate student, University of Incheon, Incheon, Korea
Jung-Oh Kim, Graduate student, University of Incheon, Incheon, Korea
Baek Youn, Samsung Electronics, Suwon, Korea

ABSTRACT: In this study, condensation heat transfer tests were conducted in flat aluminum multi-channel tubes using R-410A, and the results are compared with those of R-22. Two internal geometries were tested; one with a smooth inner surface and the other with micro-fins. Data are presented for the following range of variables; vapor quality (0.1 ~ 0.9), mass flux (200 ~ 600 kg/m^2s) and heat flux (5 ~ 15 kW/m^2). Results show that the effect of surface tension drainage on the fin surface is more pronounced for R-22 than R-410A. The smaller Weber number for R-22 may be responsible. For the smooth tube, the heat transfer coefficient of R-410A is slightly larger than that of R-22. For the micro-fin tube, however, the reverse is true. Possible reasoning is provided considering the physical properties of the refrigerants. For the smooth tube, Akers et al. (1959) type correlation predicts the data reasonably well. For the micro-fin tube, the Yang and Webb (1997) model was modified to correlate the present data. The modified model adequately predicts the data.

1. INTRODUCTION

Condensers are one of the major components comprising an air-conditioning system, and rigorous efforts have been made to improve the thermal performance of fin-and-tube type condensers. These include a usage of high performance fins, and of small diameter tubes, etc. However, fin-and-tube heat exchangers have inherent short-comings such as a contact resistance between fins and tubes, existence of low performance region behind tubes, etc. These short-comings may be overcome if fins and tubes are soldered, and low-profile flat tubes are used. Brazed flat-tube heat exchangers with aluminum louver fins, could be the choice. Such flat-tube heat exchangers have been used as condensers of automotive air-conditioning units for more than ten years.

(a) micro fin tube D_h=1.56mm

(b) smooth tube D_h=1.41mm

Figure 1. Flat Extruded Aluminum Tubes Tested in This Study.

Flat tubes are shown in Fig. 1. Typical width of flat tubes is 16 to 20 mm, and typical height is 1 to 3 mm. These tubes have rectangular sub-channels of a small hydraulic diameter (1 to 2 mm). The channel may be smooth or micro-finned. Yang and Webb(1996) and Webb and Yang (1995) conducted condensation heat transfer tests using R-12 and R-134a in smooth (D_h = 2.64 mm) and micro-finned (D_h = 1.56 mm) flat tubes. They showed that the data were reasonably predicted by the Akers et al. (1959) correlation. The data were underpredicted by the Shah (1979) correlation. The heat transfer coefficient of the micro-finned tube was 10 to 60% higher than that of the smooth tube. The difference increased with increasing vapor quality. They attributed the trend to the additional surface-tension drainage condensation on the fin surface, which is exposed to vapor at increased vapor quality. Kim et al. (2000) provided R-22 condensation data for the same flat tubes as those used by Yang and Webb (1996). They also confirmed the dominance of surface tension force at high vapor quality region.

Since the Montreal protocol, chlorofluorocarbons (CFCs) and hydrochlorofluorocarbons (HCFCs) are being substituted by potential candidates. R-22, which is widely used in household air-conditioners, is supposed to be replaced to R-410A or R-407C. Despite the high condensing pressure, R-410A has negligible gliding temperature difference (less than 0.2 K), and has been given more attention compared to R-407C. However, the literature reveals no data on R-410A condensation in flat tubes. In this study, R-410A condensation tests were conducted in two different flat tubes ; one with smooth inner surface (D_h = 1.41 mm), the other with micro-finned inner surface (D_h = 1.56 mm). The same tubes as those used by Yang and Webb (1996) and Kim et al. (2000) were tested. Cross-sectional photos of the tubes are shown in Fig. 1. The height and pitch of the micro-fin was 0.2 mm and 0.4 mm respectively. The test range covered the mass flux from 200 to 600 kg/m^2 s and the heat flux from 5 to 15 kW/m^2. The saturation temperature was maintained at 45^{0}C.

2. EXPERIMENTAL APPARATUS

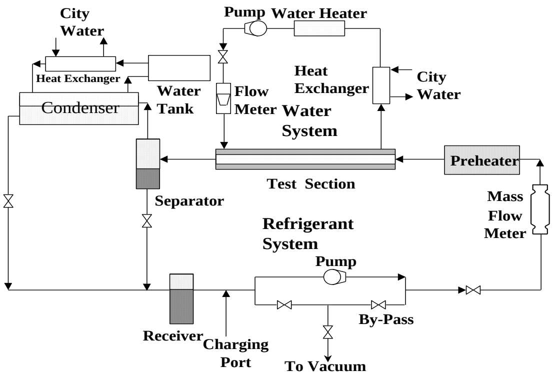

Figure 2. Schematic Drawing of the Experimental Apparatus.

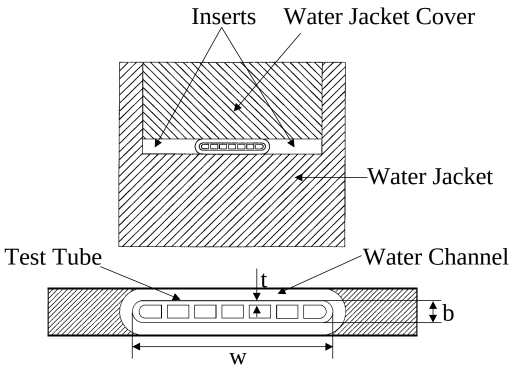

Figure 3. Detailed Drawing of the Test Section.

Table 1. Geometric Details of the Tested Flat Tubes and Corresponding Annular Channels.

		Micro-finned flat tube		Smooth flat tube	
Item		Tube	Annulus	Tube	Annulus
Tube	w(mm)	16.00	18.00	18.00	20.30
	b(mm)	3.00	5.00	1.70	4.20
	A_c(mm)	22.68	39.60	14.72	51.58
	$A_i/L(P_w)$(mm)	57.99	77.30	41.74	83.97
	D_h(mm)	1.56	2.05	1.41	2.46
	t(mm)	0.50	-	0.36	-
Fin	e(mm)	0.20	-	-	-
	p(mm)	0.40	-	-	-
	γ(deg)	40	-	-	-
	r_o(mm)	0.013	-	-	-
	r_b(mm)	0.15	-	-	-

A schematic drawing of the apparatus is shown in Fig. 2, and a detailed drawing of the test section is shown in Fig. 3. The apparatus and the test section were made similar to those used by Yang and Webb (1996). The test section comprises of a flat tube and an annular channel with a length of 455 mm. The refrigerant flows inside of the tube and the cooling water flows in the annular channel. For an accurate measurement of tube-side condensation coefficient, it is important to minimize the thermal resistance of the annular side. This was accomplished by increasing the annular-side water velocity. To increase the water velocity, the annular gap was maintained small (1.0 mm). Geometric details of tested flat tubes and corresponding annular channels are listed in Table 1.

As illustrated in Fig. 2, the refrigerant flows into the test section at a known quality and partly condenses in the test section by an annular-side cooling water. Two-phase refrigerant mixture from the test section enters the separator, where the liquid drains down to the receiver and the vapor flows into the upper shell-and-tube condenser. The condensed liquid drains down to the receiver. The sub-cooled liquid passes through the magnetic pump, mass flow meter, and enters the pre-heater. The refrigerant flow rate was controlled by by-passing an appropriate amount of liquid. The vapor quality into the test section was controlled by the heat input supplied to the pre-heater. The heat flux to the flat tube was controlled by changing the temperature of a cooling water. The flow rate of cooling water was fixed at 1.0 liter per minute throughout the test.

Temperatures were measured at five locations; refrigerant temperatures at inlet and outlet of the test tube, cooling water temperatures at inlet and outlet of the annular channel and a sub-cooled refrigerant temperature at inlet of the pre-heater. Thermowells having five thermocouples each were used to measure local temperatures. Two absolute pressures were measured - one at the inlet of the test section, and the other at inlet of the pre-heater. These absolute pressures were used to check the state (sub-cooled or saturated) of the refrigerant. A differential pressure transducer was used to measure the pressure drop across the test section. Experimental uncertainties associated with the sensors are listed in Table 2.

Table 2. Experimental Measurement Uncertainties.

Sensors	Accuracy
Temperature	60.058C
Absolute pressure	61.0%
Refrigerant flow rate	60.2%
Water flow rate	61.0%
Heat supplied to the pre-heater	61.0%

The apparatus operated at 27 atmospheric pressure corresponding to the saturation temperature 45^{0}C and was checked for leak-tight. Leak tests were conducted by a soap bubble technique followed by a halogen leak detection. The leakage resulted in a decrease in pressure less than 0.5 kPa per hour. Condensation tests started at maximum heat flux and mass flux. After the system was stabilized, quality (from 0.1 to 0.9), heat flux (from 5 to 15 kW/m^2) and mass flux (from 200 to 600 kg/m^{2}s) were sequentially varied.

3. DATA REDUCTION

The tube-side condensation coefficient h_i is determined from Eq. (1) using the overall heat transfer coefficient U_o and the annular-side heat transfer coefficient h_o. Here, A_m is the heat transfer area at the middle plane of tube wall.

$$h_i = [(\frac{1}{U_o} - \frac{1}{h_o})\frac{A_i}{A_o} - \frac{tA_i}{kA_m}]^{-1} \quad (1)$$

The annular-side heat transfer coefficient h_o was determined from the modified Wilson plot as suggested by Farrell et al. (1991). To run a Wilson plot test, it is important to maintain both the tube-side and the annular-side turbulent. To promote turbulence in the annular-side, thin wire of 0.3 mm diameter was wrapped around the tube with 3.0 mm pitch. The average vapor quality in the test tube is determined from Eq. (2)

$$x_{ave} = x_{in} - \Delta x/2 \quad (2)$$

Here, Δx is the change of vapor quality across the test section. The vapor quality into the test section is determined from Eq. (3). Here, Q_p is the heat supplied to the pre-heater and $T_{p,in}$ is the refrigerant temperature into the pre-heater.

$$x_{in} = \frac{1}{i_{fg}}[\frac{Q_p}{m_r} - c_{pr}(T_{sat} - T_{p,in})] \quad (3)$$

Experimental uncertainties were analyzed following the method by Kline and McClintock (1953). The uncertainty on the heat transfer coefficient ranged from 4.1% to 11.2%. The uncertainty increased as the vapor quality decreased.

4. RESULTS AND DISCUSSION

Fig. 4 shows the R-410A heat transfer coefficient at the mass flux 200 kg/m^{2}s. Both smooth and micro-fin data are shown. Note that the actual wetted surface area was used for the heat transfer area. Due to limitation of the apparatus, low quality data of the smooth tube were not obtainable. Fig.4 shows that the heat transfer coefficient of the micro-fin tube is higher than that of the smooth tube. This trend is consistent with that by Kim at al. (2000), who reported the R-22 data for the same tubes. Fig 5 shows the R-22 data by Kim et al. at the heat flux 10 kW/m^2. The micro-fin tube yields higher heat transfer coefficients, except for the high mass flux (600 kg/m^{2}s). At the mass flux 600 kg/m^{2}s, the heat transfer coefficients of both tubes are approximately the same. At a low mass flux, the surface tension drainage force on the fin surface may act to increase the heat transfer coefficient. At an increased mass flux, the inertial force may dominate over the surface tension force. In such case, the heat transfer coefficient of the micro-fin tube would be the same as that of the smooth tube.

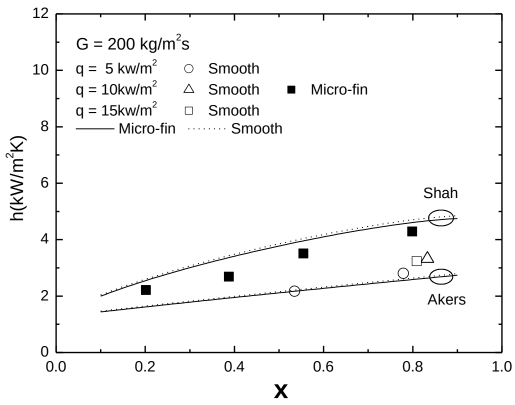

Figure 4. R-410A Condensation Heat Transfer Coefficients at G=200kg/m^{2}s.

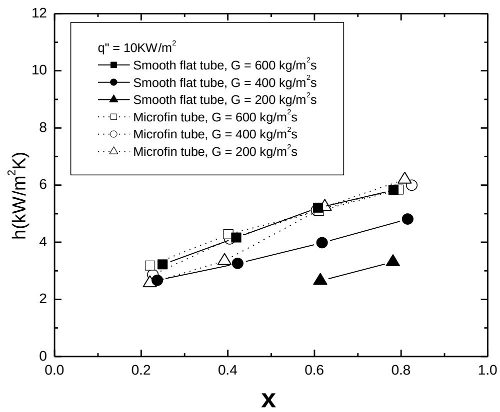

Figure 5. R-22 Condensation Heat transfer Coefficients Showing the Effect of Mass Flux.

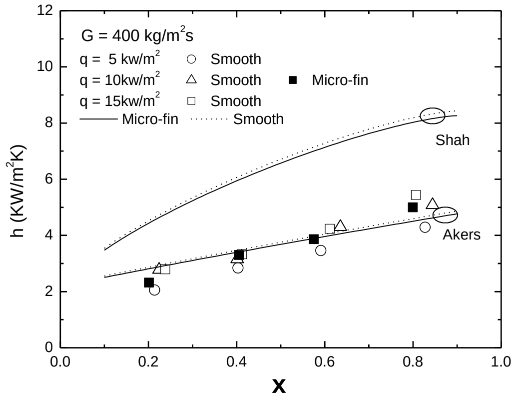

Figure 6. R-410A Condensation Heat Transfer Coefficients at G=400kg/m^{2}s.

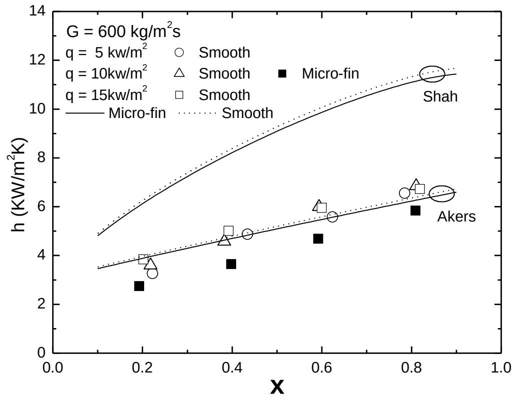

Figure 7. R-410A Condensation Heat Transfer Coefficients at G=600kg/m^{2}s.

Fig. 6 shows the R-410A results at the mass flux 400 kg/m^{2}s. The heat transfer coefficient of the micro-fin tube is approximately the same as that of the smooth tube. Fig. 6 also shows that the effect of heat flux is negligible. In Fig. 7, the mass flux 600 kg/m^{2}s data are shown. At the mass flux, the heat transfer coefficient of the smooth tube is larger than that of the micro-fin tube. Decrease of the heat transfer coefficient for finned tube has been reported by Carnavos (1979) for single-phase turbulent flow. Fins act to reduce the flow velocity in the inter-fin region, and decrease the heat transfer. For the condensation heat transfer, however, fins induce the surface drainage force, and increase the heat transfer. At a low mass flux, where the reduction of the inter-fin velocity is likely to be small and the surface tension induced enhancement is considerable, finned tubes may yield higher heat transfer coefficients than the smooth tube. At a higher mass flux, the reduction of the inter-fin velocity will be larger, and finned tubes may yield smaller heat transfer coefficients.

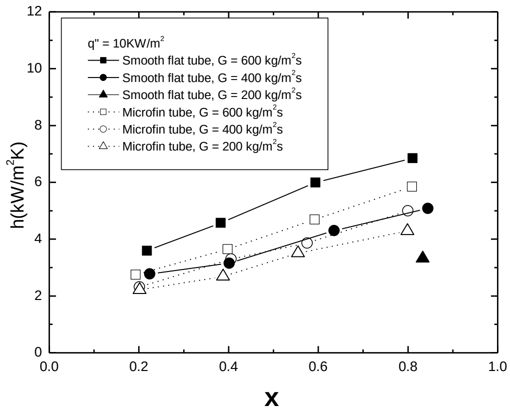

Figure 8. R-410A Condensation Heat Transfer Coefficients Showing the Effect of Mass Flux.

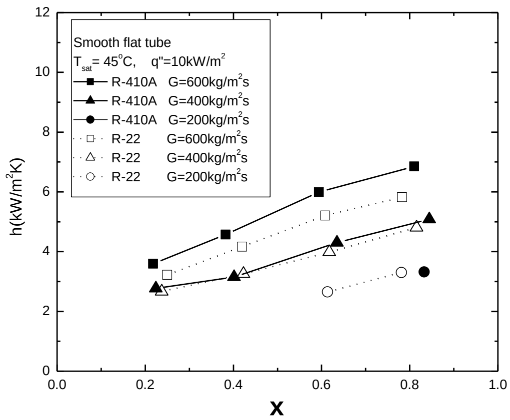

Figure 9. Condensation Heat Transfer Coefficients of R-22 and R-410A in the Smooth Tube.

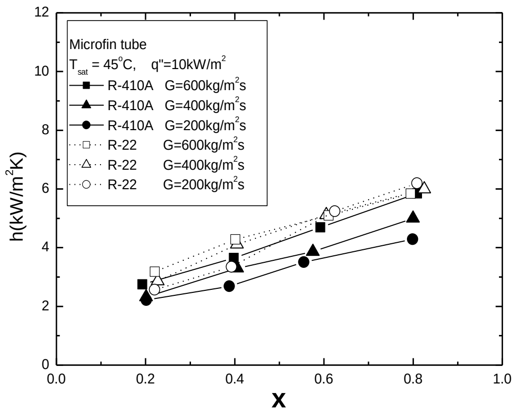

Figure 10. Condensation Heat Transfer Coefficients of R-22 and R-410A in the Micro-fin Tube.

The effect of mass flux is more clearly seen in Fig. 8. The trend on the mass flux is different from that of R-22 (Fig. 5), where the finned tube yielded higher heat transfer coefficient for the entire mass flux. The relative importance of the inertial force over the surface tension force may be obtained from the corresponding Weber number [$= G^2 D_h /(\rho_l \sigma)$]. The Weber number of R-410A is 2.7 times larger than that of R-22, which may partly explain the different fin effect between R-22 and R-410A. For R-22, which has a smaller Weber number (or stronger surface tension force), finned tubes would be more beneficial.

In Fig. 9, the heat transfer coefficients of R-410A are compared with those of R-22 for the smooth tube. The heat flux is 10 kW/m^2. The heat transfer coefficients of R-410A are slightly higher. The micro-fin data are shown in Fig. 10. For the micro-fin, R-22 yields higher heat transfer coefficients. In addition, R-22 data tend to converge at a high quality region, whereas R-410A does not show the trend. As discussed previously, R-22 has smaller Weber number, and will induce strong surface tension drainage on the fin surface, especially at a high quality region.

Previous figures suggest that the Akers et al. (1959) type equation may be used to correlate the smooth tube data. Multiple regression of the data yielded the following equation. Both R-22 and R-410A data were used for the correlation.

$$Nu_{D_h} = 0.030 \, \mathrm{Re}_{eq}^{0.78} \, \mathrm{Pr}^{1/3} \qquad (4)$$

For the micro-fin data, however, the surface tension term should be considered in addition to the vapor shear term in developing a correlation. Recently, Yang and Webb (1997) developed a semi-empirical model, which can predict the condensation coefficient in smooth or micro-fin tubes. The Yang and Webb model is listed in Table 3. Detailed description of the model is described in Yang and Webb (1997). They proposed that condensation in a smooth tube or in a micro-fin tube at low vapor quality would be controlled by vapor shear. For a micro-fin tube at high quality, where fins are exposed to vapor, they proposed that both the vapor shear and the surface tension would be important, and proposed a model which combines the two forces in an asymptotic form. For the accurate prediction of surface tension controlled heat transfer, however, the shape of liquid film, which is dependent on the fin profile, should be known. This requires a solution of complex differential equations, which is only possible by a numerical approach. Yang and Webb, instead, assumed a linear surface tension drainage force, and then introduced a correction factor, which they obtained from data-fit.

Yang and Webb recommend Akers et al.'s type correlation in the vapor shear controlled regime.

TABLE 3. Correlations cited in this study.

Reference		Correlations
Akers *et al*. (1959)		$Nu = 0.0265 \mathrm{Re}_{eq}^{0.8} \mathrm{Pr}_l^{1/3}$
Shah (1979)		$h = h_l \left[(1-x)^{0.8} + \frac{3.8x^{0.76}(1-x)^{0.04}}{P_{red}^{0.38}} \right]$ $h_l = 0.023 \frac{k_l}{D_h} \mathrm{Re}_l^{0.8} \mathrm{Pr}_l^{0.4}$
Yang and Webb (1979)		$h = h_u \frac{A_u}{A} + h_f \frac{A_f}{A}$ $h_f = 0.0265 \frac{k_l}{D_h} \mathrm{Re}_{eq}^{0.8} \mathrm{Pr}_l^{1/3}$ $h_u = \sqrt{h_{sh}^2 + h_{st}^2}$ $h_{sh} = 0.0265 \frac{k_l}{D_h} \mathrm{Re}_{eq}^{0.8} \mathrm{Pr}_l^{1/3}$ $h_{st} = C \frac{\tau_z - \tau_i}{(dp/dz)} k_l \frac{((1/r_b)-(1/r_o))}{S_m} \frac{\mathrm{Re}_{eq} \mathrm{Pr}_l^{1/3}}{We}$ $C = 0.0703$
This study (Modified Yang and Webb)	Smooth tube :	$Nu = 0.030 \mathrm{Re}_{eq}^{0.78} \mathrm{Pr}^{1/3}$
	Micro-fin tube:	Same as Yang and webb(1997) except $h_f = h_{sh} = 4.39 \frac{k_l}{D_h} \mathrm{Re}_{eq}^{0.242} \mathrm{Pr}_l^{1/3}$ $C = 0.213$

The micro-fin data at low vapor qualities (x<0.5) were used for the data-fit, which yielded the following correlation.

$$Nu_{D_h} = 4.93 \mathrm{Re}_{eq}^{0.242} \mathrm{Pr}_l^{1/3} \qquad (5)$$

The micro-fin data at high qualities (x>0.5) were also predicted by Yang and Webb's model. As mentioned, Yang and Webb introduced a correction factor 'C' to adjust the model and the data. The value C = 0.0703 fitted their data best. A different value C = 0.213, however, was determined from the present data-fit. A principal reason why a different value of 'C' is applicable here is that Yang and Webb used the Akers et al. correlation to predict the vapor shear component. The present authors believe that Eq. (5) is more appropriate. The present model (modified Yang and Webb model) is listed in Table 3. All the present data (smooth and micro-fin, R22 and R-410A) are compared with the predictions by the present model, and 81% of the data are predicted within ± 20 %.

5. CONCLUSIONS

Condensation heat transfer coefficients of R-410A were measured in a smooth and a micro-fin flat tube, and compared with those of R-22. Test range covered the mass flux from 200 to 600 kg/m^2s and the heat flux from 5 to 15 kW/m^2. The saturation temperature was 45^0C. Listed below are major findings.

1) The effect of surface tension drainage on the fin surface is more pronounced for R-22 than R-410A. The smaller Weber number for R-22 may be responsible.
2) For the smooth tube, the heat transfer coefficient of R-410A is slightly larger than that of R-22. For the micro-fin tube, however, the reverse is true. Possible reasoning is provided considering the physical properties of the refrigerants.
3) For the smooth tube, Akers et al. (1959) type correlation predicts the data reasonably well. For the micro-fin tube, the Yang and Webb (1997) model was modified to correlate the present data. The modified model predicts most of the data within ± 20 %.

Acknowledgements

Financial support from Sunmoon University (Regional Research Center for Advanced Climate Control Technology) is kindly acknowledged.

NOMENCLATURE

A	heat transfer area (mm^2)
A_c	cross-sectional flow area (mm^2)
A_i	total internal surface area (mm^2)
b	thickness of the flat tube (mm)
c_p	specific heat (J/kgK)
D_h	hydraulic diameter (mm)
e	fin height (mm)

G	mass flux (kg/m^{2}s)
G_{eq}	equivalent mass flux $= G[(1-x)+x(\rho_l/\rho_v)^{0.5}]$ (kg/m^{2}s)
h	heat transfer coefficient (W/m^{2}K)
h_f	heat transfer coefficient for finned region (W/m^{2}K)
h_{sh}	heat transfer coefficient attributable to shear force (W/m^{2}K)
h_{st}	heat transfer coefficient attributable to surface tension force (W/m^{2}K)
h_u	heat transfer coefficient for un-finned region (W/m^{2}K)
i_{fg}	latent heat of vaporization (J/kg)
j_g	superficial gas velocity (m/s)
j_g^*	dimensionless gas velocity $= \dfrac{Gx}{\sqrt{D_h g \rho_v(\rho_l - \rho_v)}}$ (-)
j_l	superficial liquid velocity (m/s)
k	thermal conductivity (W/mK)
L	length of the test section (mm)
m	mass flow rate (kg/s)
Nu_{Dh}	Nusselt number based on hydraulic diameter = hD_h/k (-)
P	pressure (N/m^2)
p	fin pitch (mm)
P_c	critical pressure (N/m^2)
P_{red}	reduced pressure $= P/P_c$ (-)
Pr	Prandtl number $= \mu c_p / k$ (-)
P_w	wetted perimeter (mm)
q	heat flux (W/m^2)
Q	heat transfer rate (W)
Re_{eq}	equivalent Reynolds number $= G_{eq}D_h/\mu_l$ (-)
Re_l	Reynolds number for liquid flow = GD_h/μ_l (-)
r_b	fin base radius (mm)
r_o	fin tip radius (mm)
S_m	length of fin profile (mm)
T	temperature (K)
t	tube wall thickness (mm)
U	overall heat transfer coefficient (W/m^{2}K)
w	width of the flat tube (mm)
We	Weber number $= G_{eq}^2 D_h /(\rho_l \sigma)$ (-)
x	vapor quality (-)

X_{tt} Martinelli parameter for turbulent-turbulent flow $= (\frac{1-x}{x})^{0.9}(\frac{\rho_v}{\rho_l})^{0.5}(\frac{\mu_l}{\mu_v})^{0.1}$ (-)

z coordinate parallel to the flow (mm)

Greek Symbols

γ apex angle of the fin (deg)

µ dynamic viscosity (kg/ms)

ρ density (kg/m^3)

σ surface tension (N/m)

τ_i wall shear stress in z direction (N/m^2)

τ_z liquid-vapor interfacial shear stress (N/m^2)

Subscripts

ave average

meas measured

eq equivalent

f finned

i tube-side

in inlet

l liquid

m mean

o annular-side

out outlet

p pre-heater

pred predicted

r refrigerant

sat saturation

u un-finned

v vapor

v vapor

REFERENCES

Akers W.W., Deans H.A. and Crosser O.K. 1959. Condensation heat transfer within horizontal tubes, Chem. Eng. Progress Symp. Series, Vol. 55(29), pp. 171-176.

Carnavos T.C. 1979. Cooling air in turbulent flow with internally finned tubes, Heat Transfer Engineering, Vol. 1(2), pp. 41-46.

Farrell P., Wert K. and Webb R.L. 1991. Heat transfer and friction characteristics of turbulator radiator tubes, SAE Technical Paper Series 910197.

Kim N-H., Cho J-P. and Kim. J-O. 2000. R-22 condensation in flat aluminum multi-channel tubes, J. Enhanced Heat Transfer, Vol. 7, pp. 427-438.

Kline S.J. and McClintock F.A. 1953. The description of uncertainties in single sample experiments, Mechanical Engineering, Vol. 75, pp. 3-9.

Shah M.M. 1979. A general correlation for heat transfer during film condensation in tubes, Int. J. Heat Mass Transfer, Vol. 22(4), pp. 547-556.

Webb R.L. and Yang C-Y. 1995. A comparison of R-12 and R-134a condensation inside small extruded aluminum plain and micro-fin tubes, C4961053195, IMechE, pp. 77-86.

Yang C-Y. and Webb R.L. 1996. Condensation of R-12 in small hydraulic diameter extruded aluminum tubes with and without micro-fins, Int. J. Heat Mass Trans., Vol. 39(4), pp. 791-800.

Yang C-Y. and Webb R.L. 1997. A predicted model for condensation in small hydraulic diameter tubes having axial micro-fins, J. Heat Trans., Vol. 119, pp. 776-782.